



Palladium Nanoparticles-Decorated β -Cyclodextrin–Cyanoguanidine Modified Graphene Oxide: A Heterogeneous Nanocatalyst for Suzuki–Miyaura Coupling and Reduction of 4-Nitrophenol Reactions in Aqueous Media

Haniyeh Daneshafruz¹ · Hossein Barani² · Hassan Sheibani¹

Received: 29 July 2021 / Accepted: 21 December 2021 / Published online: 7 January 2022

© The Author(s), under exclusive licence to Springer Science+Business Media, LLC, part of Springer Nature 2021

Abstract

In this study, graphene oxide used as a stable support to adsorb and stabilize palladium nanoparticles for preparing a heterogeneous nanocatalyst. In order to increase the palladium adsorption, the surface of graphene oxide was functionalized with β -Cyclodextrin and cyanoguanidine compounds. The prepared nanocatalyst was defined by various characterization techniques such as FT-IR, XRD, TEM, SEM–EDX, ICP and UV–Vis. The catalytic efficiency of the synthesized organic–inorganic nanocomposite investigated by focusing on the Suzuki–Miyaura binding reaction and reduction of 4-nitrophenol to 4-aminophenol, which the nanocatalyst work is easy, affordable, and environmentally safe. The performed reaction showed high yields of biphenyl compounds through the Suzuki–Miyaura reaction and confirms very good conversion of 4-nitrophenol to its reduced form. Also, the proposed nanocatalyst presented significant catalytic efficiency (yield: 98% to 91%) after using five times.

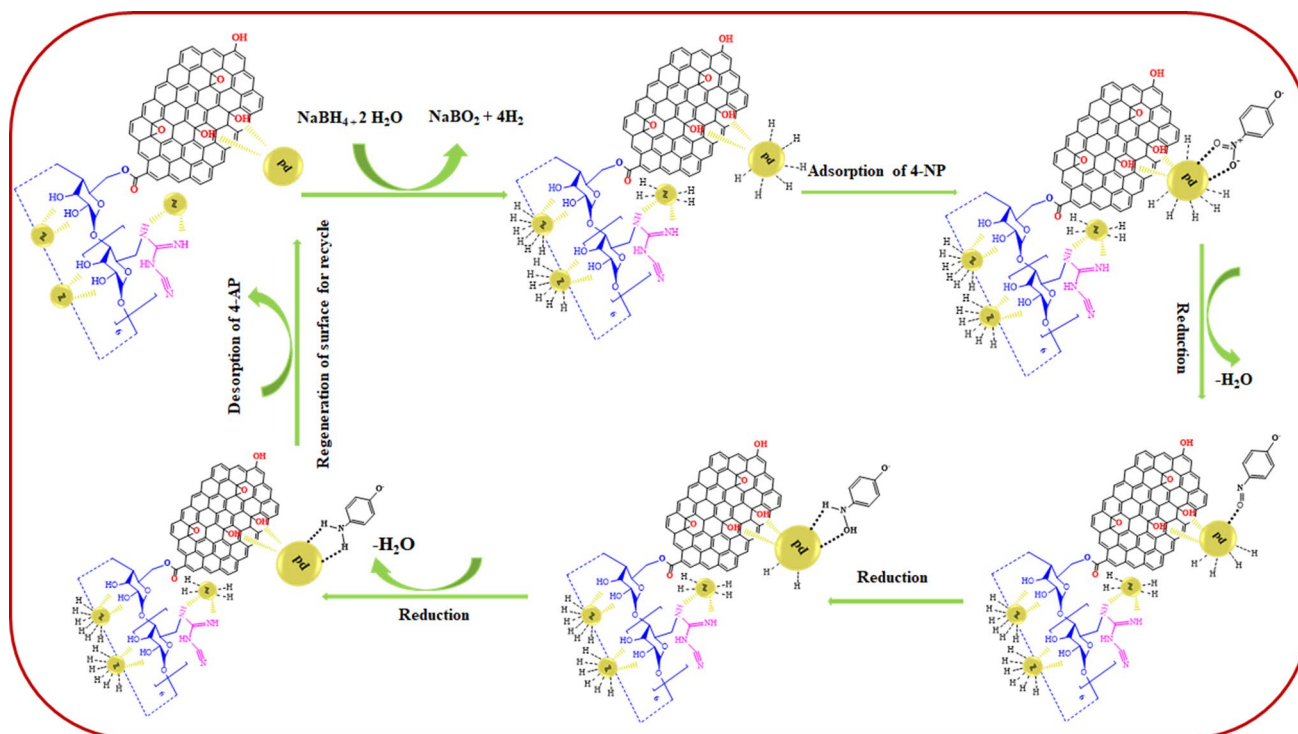
✉ Hossein Barani
barani@birjand.ac.ir

✉ Hassan Sheibani
hsheibani@uk.ac.ir

¹ Department of Chemistry, Shahid Bahonar University of Kerman, 76169 Kerman, Iran

² Department of Carpet, University of Birjand, 17 Shahrivar Street, Birjand, Iran

Graphical Abstract



Keywords Graphene oxide · Palladium nanoparticles · β -Cyclodextrin · Suzuki–Miyaura · 4-Nitrophenol

1 Introduction

In chemistry today, with the help of powerful reactions such as crosslinking, biologically active molecules and complex compounds can be synthesized. Based on these potential reactions can be taken vital steps in the pharmaceutical and agricultural industries [1]. Among them, Suzuki–Miyaura and Mizoroki–Heck reactions are the most important and valuable cross-linking reactions [2]. These two important reactions, further being effective in the drugs development such as Morphine [3], (+) Dynemicin [4], and Paclitaxel (Taxol) [5] in the pharmaceutical industry, can also play a key role in eliminating many harmful human activities to the environment. Another issue of great technical and scientific importance is the removing or reducing nitro-aromatic compounds from aqueous media. These compounds are widely used in many industries, from the production of dyes, aniline, paper, explosives, and pesticides to the preparation and production of medicine [6–8], so they are one of the main groups of aquatic pollutants [9, 10]. According to this, the use of a new generation of catalysts can be effective. The wide range of advantages and applications of Pd-based catalysts forming C–C bonds has led to their continued consideration. However, designing and selecting

recyclable and environmentally friendly catalysts that can be highly efficient in industrial applications for specific reactions is still challenging for researchers [11–15]. According to previous studies, the use of homogeneous catalysts is not desirable due to their non-recyclability nature and the contamination probability of reaction products by the metals used in the catalyst [16, 17]. Therefore, an attempt was made to solve this problem by using heterogeneous catalysts in which palladium particles have been fixed on various solid substrates, including activated carbon [18, 19], zeolites [20], and polymers [21, 22].

Although the heterogeneous catalysts are easily recyclable, they cannot perform as well as homogeneous catalysts [23, 24]. Therefore, recently the design of ideal recycled nanocatalysts has received much attention due to their stability and high efficiency [25–30].

In recent years, graphene has emerged as a suitable substrate for metal nanoparticles with good stabilizing power and dispersion in the synthesis of nanocatalysts [30–33], which its derivatives with a variety of organic and inorganic ligands has been used in many studies [34, 35]. Graphene oxide (GO) is one of the most important derivatives of graphene and its properties such as high surface area, high thermal stability, inertness, and having functional groups

such as hydroxyl, epoxy, and carboxyl which have made it as a supstra with significant adsorption capacity and ideal option in the construction of nanocatalysts [36]. In addition, becoming composite is another unique feature of graphene and its derivatives. They can easily decorated with diverse functional groups or nanomaterials and enhance the performance of the designed nanocatalyst [37, 38].

Cyclodextrins (CDs) are a family of cyclic oligosaccharides, consisting of a macrocyclic ring of glucose subunits joined by α -1,4 glycosidic bonds with various industrial applications since the end of the 1980s in the field of medicine, supramolecular and catalysis chemistry [39–44]. Being biodegradable, nontoxic, available, producible in large scale amounts, easily functionalized, having a hydrophobic central cavity and hydrophilic outer surface, and stability against chemical and photochemical degradation are some of the advantages of CDs that make them a good candidate for the above applications [45–49].

In this project, a new nanocatalyst designed and synthesized based on stabilized palladium nanoparticles on pre-functionalized GO with β -Cyclodextrin (β -CD) and cyanoguanidine (CG), which are abundant, non-toxic, and available substances. CG is rich in nitrogen, so it can be an excellent ligand for the chelation of Pd nanoparticles. The characteristics of synthesized nanocatalyst was determined using spectral data of FT-IR, XRD, TEM, SEM-EDX, ICP and UV-Vis. After that, its catalytic efficiency was investigated in the Suzuki–Miyaura reaction, which is a valuable reaction in the construction of carbon-carbon bonds and can to reduce the 4-nitrophenol (4-NP) to 4-aminophenol (4-AP), which is a useful and non-toxic compound. In addition, the recyclability of the new nanocatalyst was studied.

2 Experimental

2.1 Materials

All the required chemicals, including graphite, sulfuric acid (H_2SO_4), sodium nitrate (NaNO_3), potassium permanganate (KMnO_4), hydrochloric acid (HCl), thionyl chloride (SOCl_2), dichloromethane (CH_2Cl_2), β -Cyclodextrin, benzenesulfonyl chloride, cyanoguanidine, palladium chloride (PdCl_2), phenylboronic acid, iodobenzene, bromobenzene, chlorobenzene, sodium borohydride (NaBH_4), ethanol, 4-nitrophenol (4-NP) and acetonitrile (MeCN) were purchased from Merck and Aldrich companies and used as a received.

2.2 General Procedure for Preparation of Graphene Oxide (GO)

GO was prepared from graphite powder based on modified Hummer's method [20]. According to this method, the graphite powder (2 g), sodium nitrate (1.5 g), were added in 70 mL of 98% H_2SO_4 and gently mixed in an ice bath. Then potassium permanganate (8 g) was added to the stirring mixture very slowly for controlling the reaction temperature lower 20 °C and stirring was followed for 2 h at this temperature. After that, the reaction mixture was stirred continuously for 30 min at 35 °C. Then, 100 mL of deionized water was gradually added to the thick paste obtained at 90 °C. By adding hydrogen peroxide (20 mL, 30%), the black color of suspension changed to dark green. This mixture was stirred continuously for 24 h. After that, the suspension was placed in an ultrasonic homogenizer for one hour. The resulting suspension was washed with hydrochloric acid (3%) and centrifuged four times. After that, the mixture was washed with distilled water until the pH was adjusted to 7. Finally, the aqueous dispersion of GO was dried in a vacuum oven at 60 °C for 50 h. The synthesized GO powder was stored in a container under a nitrogen atmosphere for later process.

2.3 Synthesis of GO/ β -Cyclodextrin (β -CD)

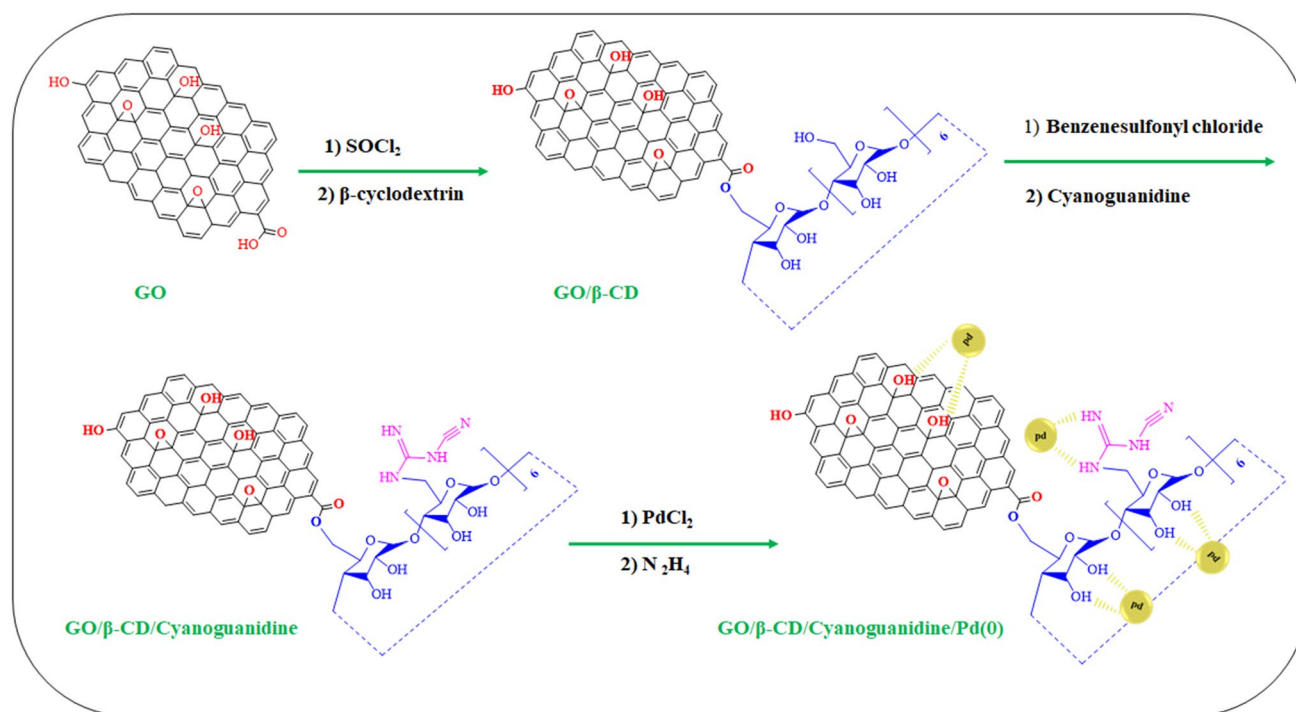
Initially, the 0.5 g of GO was refluxed with of thionyl chloride (30 mL) at 50 °C for 24 h. After that, the resulting residue was washed three times with dry dichloromethane, then dried at room temperature. Meanwhile, the β -CD (0.06 g) was refluxed with dry CH_2Cl_2 (50 mL) in a flask at 50 °C for 1 h, the previous prepared composition (0.2g; GO/ SOCl_2) was added and refluxing followed for 24 h. Finally, the resulting mixture was washed and dried twice with ethanol.

2.4 Synthesis of GO/ β -CD/Cyanoguanidine (CG)

The prepared GO/ β -CD (0.2 g) was mixed with CH_2Cl_2 (40 mL) and stirred in an ice-bath for 20 min. Then, the diluted benzenesulfonyl chloride (0.3 mL) in CH_2Cl_2 (5 mL) was added dropwise to the prepared suspension by a syringe and refluxed for 24 h. The resulting mixture was washed once with CH_2Cl_2 and dried at room temperature. The prepared powder (0.15 g) and CG (2 mmol) was added to DMSO (40 mL) and stirred for 24 h at 60 °C. Finally, the obtained composite was washed twice with ethanol and dried at room temperature.

2.5 Synthesis of GO/ β -CD/CG/Pd Nanocatalysts

In order to prepare the heterogeneous nanocatalyst (Scheme 1), firstly palladium (II) chloride (0.03 g) was dissolved in acetonitrile (70 mL), while stirred for 2 h and the



Scheme 1 Synthesis process of GO/β-CD/CG/Pd nanocatalyst

color of solution changed to a clear yellow. Also, in a separate procedure, the pre-functionalized GO/β-CD/CG (0.15 g) was added in acetonitrile (50 mL) and stirred for 30 min at 50 °C. Then the prepared palladium and pre-functionalized GO/β-CD/CG solution were added together and stirred under reflux for 24 h. After that, 1 mL of hydrazine hydrate ethanolic (1:10; v/v) solution was injected into the above reflux reaction mixture. After 6 h, the synthesized nanocatalyst was separated by centrifugation and washed twice with ethanol. Finally, the nanocatalyst dried at room temperature.

2.6 Characterization of GO/(β-CD)/(CG)/Pd Nanocatalyst

FT-IR analysis was used to evaluate the presence of functional groups in the synthesized nanocatalyst. These spectra were recorded by a commercial spectrophotometer (Bruker Tensor 27 FT-IR). The morphology of synthesized nanocatalyst sample was observed using Scanning Electron Microscope (SEM; TESCAN MIRA III) with gold-plated equipped with scattered X-ray spectroscopy. Also, TEM (Transmission Electron Microscope) was used to analyze the internal morphology of the synthesized catalyst. The crystal structure of nanocatalyst sample was determined using an X-ray diffractometer (Panalytical X'PertPro, Netherlands) with CuKα radiation ($\lambda = 1.5404 \text{ \AA}$).

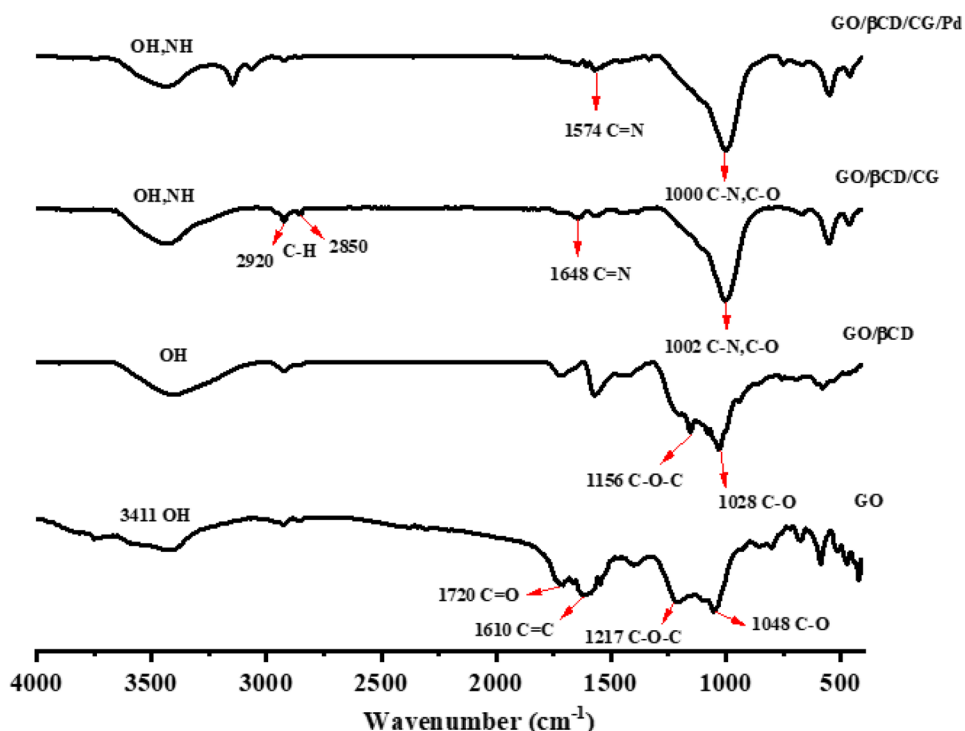
2.7 Suzuki–Miyaura Reaction Procedure

Catalyst (3 mg), arylhalide (0.5 mmol, 0.5 equiv.), phenylboronic acid (0.073 g, 0.6 mmol, 0.6 equiv.), potassium carbonate (0.06 g, 2.0 mmol) and 2 mL of EtOH/H₂O (v/v = 1: 1) were mixed in a round bottom flask. The mixture was stirred at high speed for 10 min at 60 °C. The end of the reaction was determined by thin-layer chromatography (TLC). At the end of the reaction, the catalyst was recovered using a centrifuge and the product was extracted with dichloromethane. The organic layers were dried over anhydrous Na₂SO₄ and so the solvent was removed under vacuum. The products were purified using a short column of silica gel by washing solvent such as n-hexane.

2.8 General Procedure for 4-NP Reduction

To evaluate the catalytic performance of GO/β-CD/CG/Pd nanocatalyst, the freshly solution of 4-NP (2.5 mM) and NaBH₄ (2.5 mM) was prepared. Then, the 0.5 mL of NaBH₄ and 0.1 mL of 4-NP were mixed with 4 mL of distilled water by magnetic stirring and finally transferred to a quartz cuvette. To initiate the reaction, 1 mg of catalyst was added to the cuvette, then to monitor the reduction of 4-NP to 4-AP, the absorption intensity of 4-NP at 400 nm excitation wavelength was recorded by a visible ultraviolet (UV-Vis) spectrophotometer.

Fig. 1 Normalized FTIR spectra of GO, GO/ β -CD, GO/ β -CD/CG, GO/ β -CD/CG/Pd nanocatalyst



3 Results and Discussion

3.1 FT-IR Spectra

The FTIR spectrum of the synthesized GO sample (Fig. 1) shows some characteristic signals, which are around 1048cm^{-1} (C–O stretching vibration due to C–O–C), 1217 (C–O stretching vibration due to C–OH from alcohol groups), 1610 (C=C stretching vibration of aromatic rings), 1720 (C=O stretching vibration), and the broad peak at 3411cm^{-1} (OH stretching vibration due to the hydroxyl and carboxyl functional groups). According to previous studies, the presence of bands assignable to the oxygen-containing functional groups confirms that the oxidation reaction of graphite was successfully done [50, 51]. In the synthesized GO/ β -CD spectrum, peaks 1028cm^{-1} and 1156cm^{-1} are characteristic of C–O stretching vibration (induced by O–H and C–O) in the saccharide structure [52]. In the GO/ β -CD spectrum modified with CG (GO/ β -CD/CG) peaks at 1648cm^{-1} (C=N stretching vibration), 1002cm^{-1} (C–N and C–O stretching vibration), 2850cm^{-1} and 2920cm^{-1} (C–H stretching vibrations) is specified. In addition, the wide peak in the area of 3400cm^{-1} is related to the O–H and N–H stretching vibration [53]. The last FTIR spectrum shows the synthesized nanocatalyst spectrum and the presence of Pd nanoparticles on the GO/ β -CD/CG substrate. According to this spectrum, all the adsorbed bands are transmitted at lower frequencies, which indicates that palladium metal has deposited on the composite [54].

3.2 Electron Microscopy and Elemental Analysis

According to the images obtained from SEM-EDX (Fig. 2), it is quite clear that a significant amount of Pd nanoparticles is distributed on the surface of GO sheets (Fig. 2a). Also, the presence of a strong EDX peak at 3 keV confirms the presence of Pd elements (Fig. 2b). Also, the EDX analysis has confirmed the presence of other elements such as carbon, oxygen and nitrogen. The results prove that the presence of β -CD and CG compounds have been effective in stabilizing palladium nanoparticles on the catalyst surface. On the other hand, the amount of 9.214% of palladium metal on GO/ β -CD/CG composite was measured and determined by plasma induced analysis (ICP), which is in agree with EDX results. Moreover, to further describe the synthesized nanocatalyst sample, the elemental mapping patterns was quantified (Fig. 2c), and the presence of Pd nanoparticles with good dispersion is clearly distinguishable. Also, catalyst recovery was done after 5 times of the Suzuki reaction, the analysis of FESEM and EDX were done, the results showed that the morphology and structure of the catalyst were stable. The layer structure of GO and Pd nanoparticles is well illustrated (Fig. 2d, e).

Figure 3 shows the layers of GO plates on top of each other and its edges at a scale of 100 nm. According to that, the average diameter of palladium nanoparticles have been determined around 3.2 nm (Fig. 3). It also shows that the presence of β -CD and CG in the structure of composite causes uniform distribution of palladium particles.

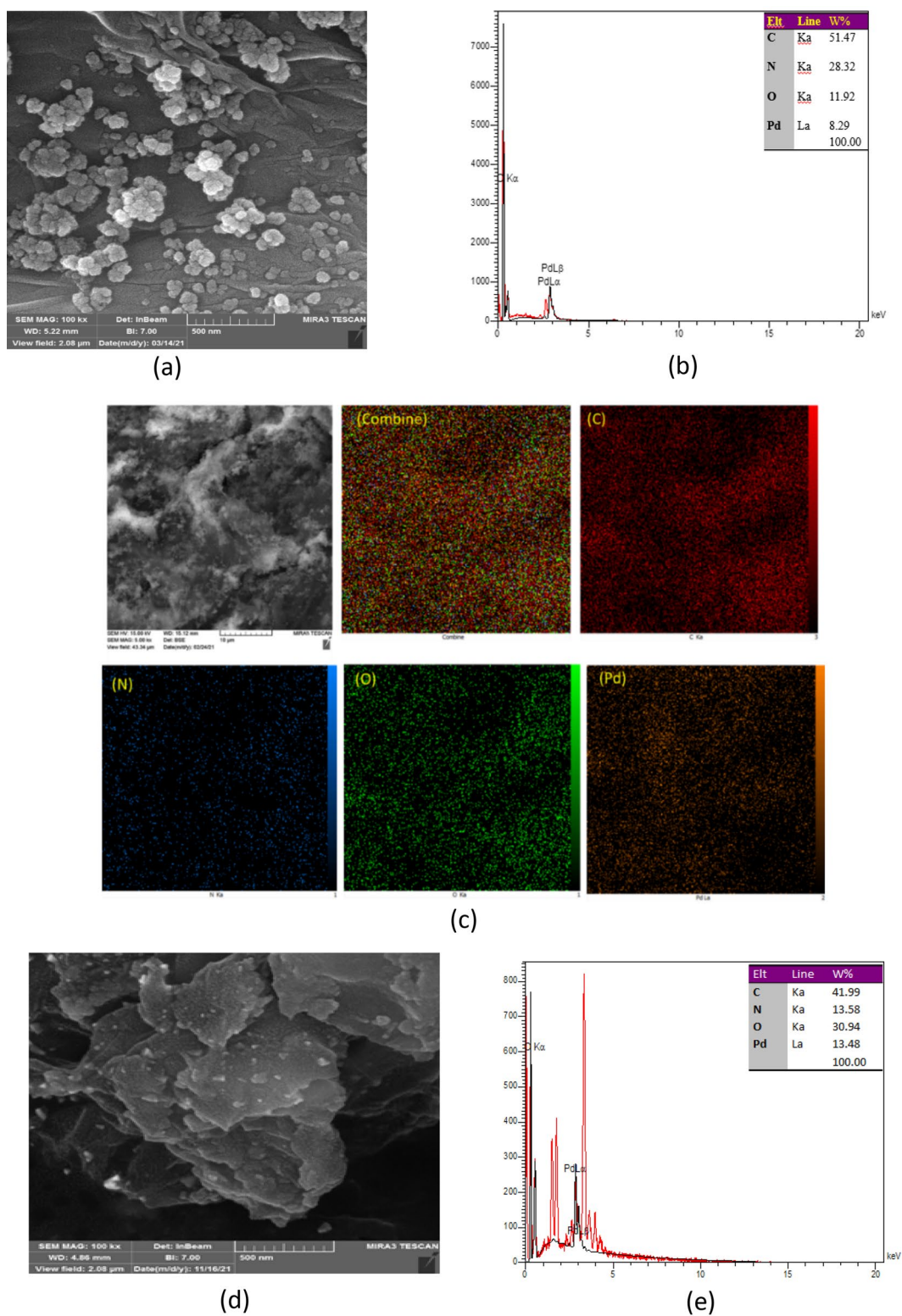


Fig. 2 SEM image of **a** GO/β-CD/CG/Pd nanocatalyst, **b** corresponding EDX spectrum, **c** elemental mapping patterns of C, N, O and Pd atoms, and **d** SEM image of nanocatalyst after recovery, and **e** EDX spectrum of nanocatalyst after recovery

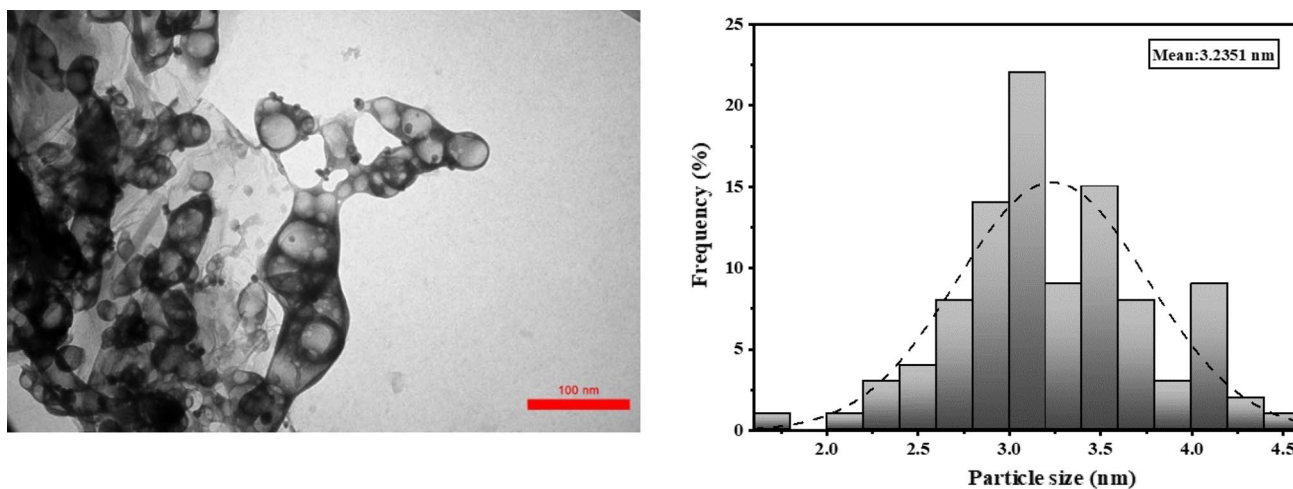


Fig. 3 TEM image of synthesized GO/β-CD/CG/Pd nanocatalyst (left) and their diameter distributions (right)

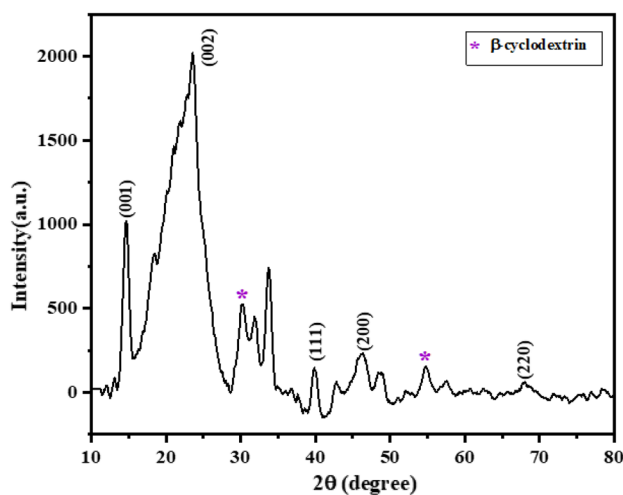


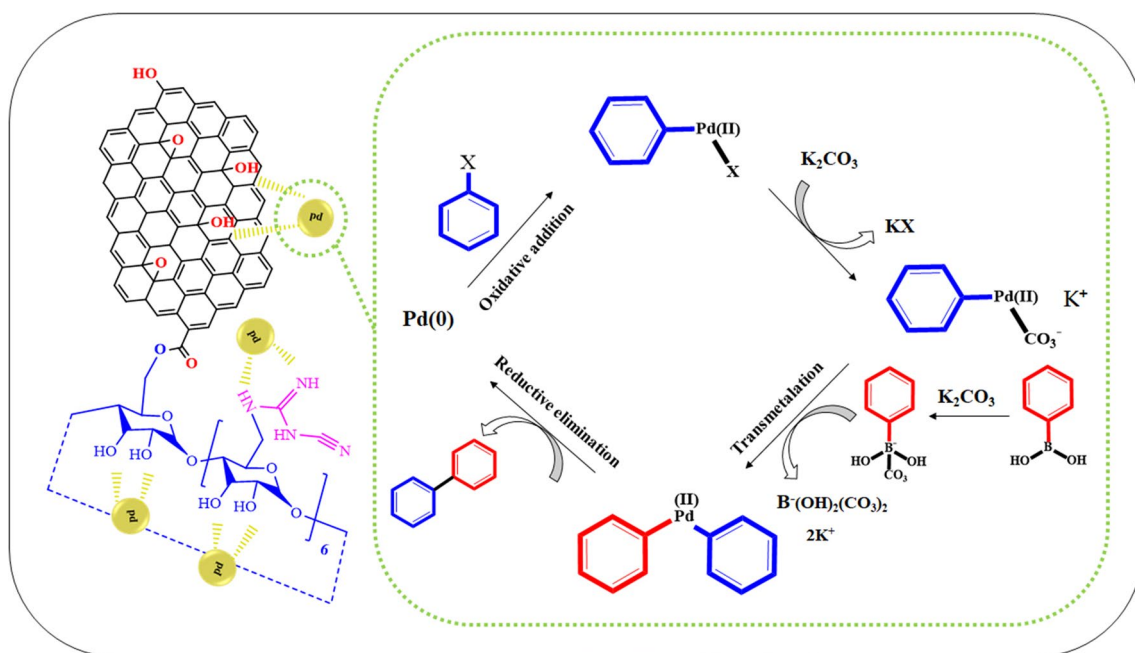
Fig. 4 XRD pattern of GO/β-CD/CG/Pd nanocatalyst

3.3 XRD Pattern Analyze

Figure 4 shows the XRD pattern of the synthesized nanocatalyst. The peak at $2\theta = 14.5^\circ$ corresponds to the (001) reflection of GO, and the peak at 23.5° (002) is broad, which can be attributed to the corrugated structure of the GO and reduced GO (rGO) sheet [55]. On the other hand, the peaks at 2θ values of 39.7° (111), 46.4° (200), and 67.2° (220) are compatible with the standard XRD data for Pd (JCPDS 46-1043) [56]. The peaks at 30.2° and 54.6° were matching with the crystal structure of the β-CD [57].

3.4 Catalytic Activity of GO/(β-CD)/(CG)/Pd for Suzuki–Miyaura Reactions

The Suzuki C–C coupling reaction was optimized based on the reaction parameters (Scheme 2) such as reaction time, solvent type, temperature, and amount of nanocatalyst. For this optimization, the coupling reaction between phenylboronic acid and iodobenzene was used. The optimal conditions were determined as follows: Nanocatalyst (3 mg), arylhalide (0.5 mmol, 0.5 equiv.), phenylboronic acid (0.073 g, 0.6 mmol, 0.6 equiv.), potassium carbonate (0.06 g, 2.0 mmol) and 2 mL of EtOH/H₂O (v/v = 1:1) at 60 °C for 10 min (Table 1, run 6). Our observations showed that the presence of a nanocatalyst in this reaction is necessary and the reaction cannot take place without it (Table 1, run 1). The various temperature was tested (40, 60, and 80 °C). The 60 °C was determined as an optimal reaction temperature among the various applied temperatures and evaluated with high performance (Table 1, run 3). As the reaction temperature increased, its time decreased. This result can be related to the reaction activation energy. Then, to find out the most effective solvent, several different solvent systems were investigated, among which a mixture of water and ethanol solvent (1:1) with high yield and efficiency (98%) was determined as the best solvent (Table 1, run 6, 11–16). The precursors of the Suzuki reaction (Aryl halide and phenylboronic acid) are soluble in ethanol, on the other hand, K₂CO₃ is soluble in the water therefore the mixture of miscible solvents can be created the best condition for the reaction. In the reaction, two bases of triethylamine and K₂CO₃ were used, which showed a low efficiency for the base of trimethylamine, which could be due to its low solubility in the solvent, but the use of K₂CO₃ showed good performance in the reaction. Therefore, K₂CO₃ was selected as the base



Scheme 2 Possible mechanism of Suzuki coupling reaction catalyzed by GO/β-CD/CG/Pd nanocatalyst

Table 1 Optimization of conditions in the Suzuki–Miyaura coupling reaction

Run	Catalyst (mg)	Base	Solvent	T (°C)	Time (min)	Yield (%) ^a
1	0	K ₂ CO ₃	EtOH/H ₂ O (1:1)	80	20	0
2	5	K ₂ CO ₃	EtOH/H ₂ O (1:1)	80	10	98
3	5	K ₂ CO ₃	EtOH/H ₂ O (1:1)	60	10	98
4	5	K ₂ CO ₃	EtOH/H ₂ O (1:1)	40	35	74
5	3	K ₂ CO ₃	EtOH/H ₂ O (1:1)	80	15	98
6	3	K ₂ CO ₃	EtOH/H ₂ O (1:1)	60	15	98
7	3	K ₂ CO ₃	EtOH/H ₂ O (1:1)	40	35	63
8	2	K ₂ CO ₃	EtOH/H ₂ O (1:1)	80	10	70
9	2	K ₂ CO ₃	EtOH/H ₂ O (1:1)	60	10	63
10	2	K ₂ CO ₃	EtOH/H ₂ O (1:1)	40	25	52
11	3	K ₂ CO ₃	EtOH	60	20	50
12	3	K ₂ CO ₃	MeCN	60	20	61
13	3	K ₂ CO ₃	DMF	60	20	70
14	3	K ₂ CO ₃	THF	60	20	40
15	3	K ₂ CO ₃	H ₂ O	60	20	50
16	3	K ₂ CO ₃	DMSO	60	20	65
17	3	No base	EtOH/H ₂ O (1:1)	60	20	3

Reaction condition: Iodobenzene 0.5 mmol, phenylboronic acid 0.6 mmol, base 0.4 mmol, catalyst, solvent (2 mL)

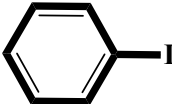
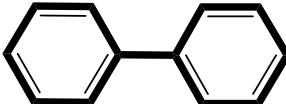
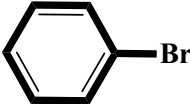
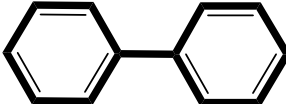
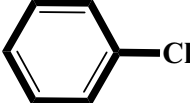
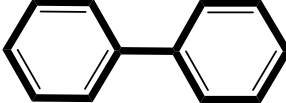
^aIsolated yield

for the Suzuki reaction. Also, the effect of the base (K₂CO₃) role in advancing the Suzuki–Miyaura coupling reaction was studied and the results showed that the reaction would not take place in its absence (Table 1, run 17).

Finally, to optimize the amount of nanocatalyst, the reaction was performed in the presence of different amounts of

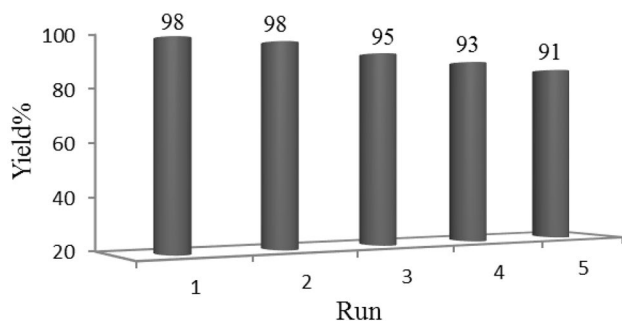
it (5, 3 and 2 mg), in which 3 mg of nanocatalyst showed the best results and performance (Table 1, run 2–10). Different aryl halides such as iodobenzene, bromobenzene and chlorobenzene have been studied under optimal conditions and the results of their study are shown in Table 2.

Table 2 C–C coupling of various aryl halides in the presence of GO/ β -CD/CG/Pd nanocatalyst under optimal condition

Run	Ar–X	Product	Yield ^a %
1			98
2			90
3			80

Reaction condition: 0.5 mmol of aryl halide, 0.6 mmol phenylboronic acid, 0.4 mmol K_2CO_3 in 2 ml solvent (EtOH/ H_2O :1:1), and in the presence of 3 mg GO/(β -CD)/(CG)/Pd catalysts at 60 °C for 10 min

^aIsolated yield

**Fig. 5** Recyclability of GO/ β -CD/CG/Pd nanocatalyst

The yield of iodobenzene coupling was more than bromobenzene and chlorobenzene (Table 2). This result is due to the weaker bond of the C–I relative to the C–Br and C–Cl.

After monitoring the Suzuki–Miyaura reaction and finally recovering the nanocatalyst by centrifugation, it was washed several times with water and ethanol and reused to evaluate its reusability. This evaluation showed (Fig. 5) that the performance of the nanocatalyst decreases very slightly even after 5 nanocatalyst cycles. ICP analysis was performed to evaluate the stability of the prepared nanocatalyst. The results show that the percentage of Pd is 4.22 (4.22% w/w). Considering the good reaction efficiency after 5 times and the ICP results, it can be concluded that the catalyst is relatively stable.

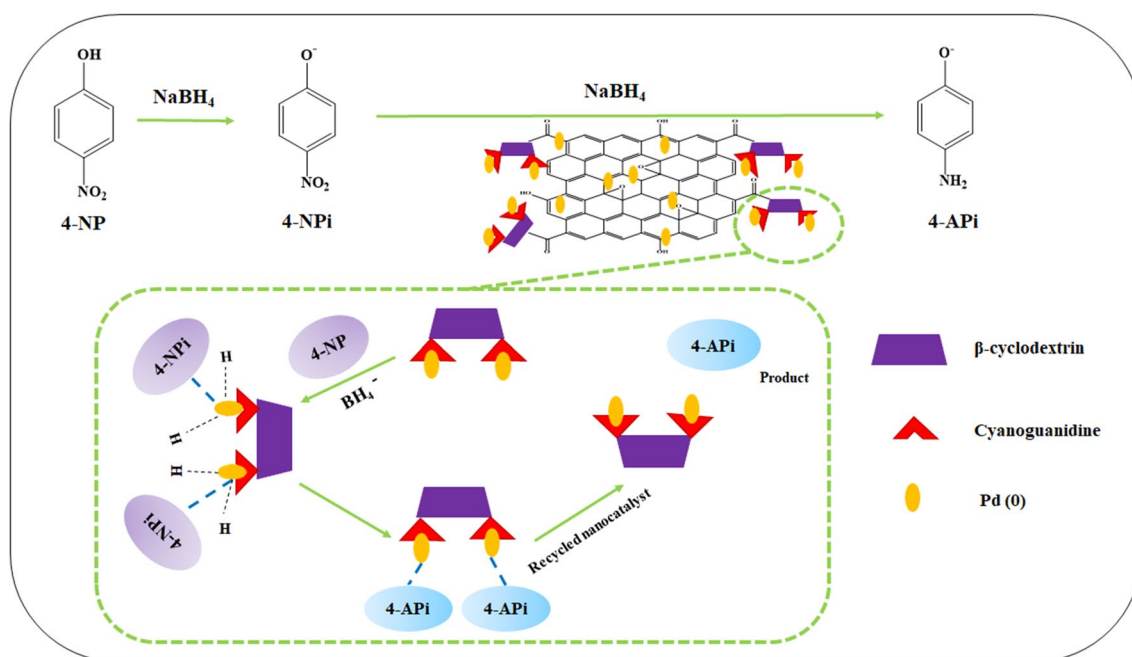
3.5 Catalytic Activity of GO/ β -CD/CG/Pd to Reduce 4-Nitrophenol

The catalytic performance of GO/ β -CD/CG/Pd for reduction of 4-NP to 4-AP was investigated in the presence of $NaBH_4$ as a reducing agent at room temperature. The reaction process (Scheme 3) was investigated using UV-Vis absorption

spectroscopy. Without the use of nanocatalysts, no change in the absorption wavelength of 4-NP was observed. After adding 1 mg of the synthesized nanocatalyst, the color of the solution changed from yellow to colorless as the reaction progressed. Also, the absorption wavelength gradually disappeared at 400 nm for 4-NP and a new peak appeared at 300 nm for 4-AP (Fig. 6). In this reaction, an excess of reagent was used to be able to define the rate of reduction reaction independently of the amount of $NaBH_4$ reagent. As a result, the 4-NP reduction reaction was considered a first-order equation, and a linear relationship between reaction time and $\ln(I/I_0)$ was defined. Finally, according to the defined relation of the reaction rate constant, K , was obtained $0.0468\ s^{-1}$. Then, by dividing the reaction rate constant by the amount of nanocatalyst used, the nanocatalyst activity parameter ($K_a = k/m$) for the GO/ β -CD/CG/Pd nanocatalyst was calculated to be $46.8\ s^{-1}\ g^{-1}$.

The beta-cyclodextrin molecule in the catalyst plays an important role in reducing 4-NP to 4-AP. Beta-cyclodextrin induces host-guest interaction with 4-NP; in the next step, 4-AP is released as a reducing product. Beta-cyclodextrin was then vacated. Finally, vacated beta-cyclodextrin is prepared to capture the 4-NP again. The "capture-reduction reaction-release" process continued until all 4-NP molecules were converted to 4-AP. Host-guest interactions can create an efficient substrate and release the reaction product by a non-covalent interaction mechanism, this advantage can be a good efficiency for the catalytic process [58, 59].

The designed catalyst functionalized with β -CD and CG to increase in loading of Pd nanoparticles and also their high stability, so this catalyst could be good results present because of the presence of many functional groups such as $-OH$ and $-NH_2$, etc. On the other hand, graphene oxide as the two-dimensional nanostructure with many functional groups could be an excellent substrate for β -CDs and CG.



Scheme 3 Possible mechanism for the catalytic reductions of nitrophenol compounds by recyclable GO/β-CD/CG/Pd nanocatalyst

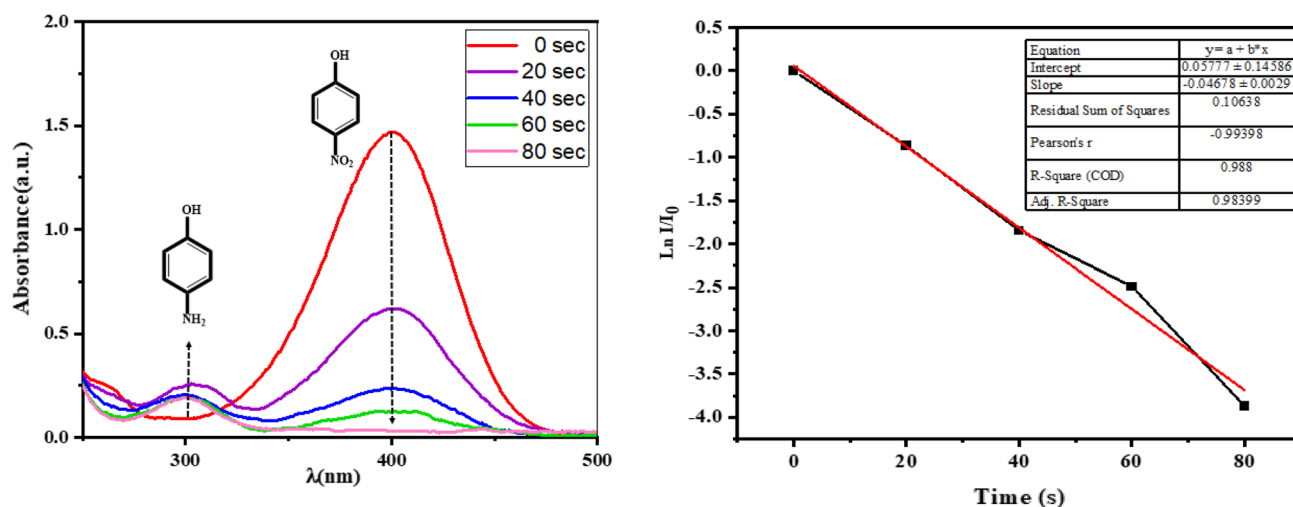


Fig. 6 The UV–visible spectra for catalytic reduction of 4-NP to 4-API (left), and plot of the Ln (I/I_0) against the different reaction times (right)

4 Conclusions

In this study, we were able to present a new method for the synthesis of recyclable nanocatalyst GO/β-CD/CG/Pd in which GO was used as a highly efficient substrate for Pd heterogeneity at the nanoparticle surface. The properties of the synthesized nanocatalyst by XRD, FT-IR, SEM, TEM, ICP, and EDX techniques confirmed the successful performance of GO sheets and the homogeneous dispersion of

Pd nanoparticles on the modified sheets. Also, the catalytic activity of the newly prepared nanocatalyst in the C–C coupling reaction was investigated using aryl halide and phenylboronic acid (Suzuki reaction) and showed that the proposed nanocatalyst is a useful tool for the preparation of biphenyl compounds. In addition to cross-linking reactions, the reduction of 4-NP to 4-API in water was applied at room temperature and the nanocatalyst was reused several times without any significant decrease in the activity.

Declarations

Conflict of interest The authors have no conflict of interest to declare.

Ethical Approval This article does not contain any studies with human participants or animals performed by any of the authors.

References

1. A. Alimardanov, L. Schmieder-van de Vondervoort, A.H. de Vries, J.G. de Vries, Use of “homeopathic” ligand-free palladium as catalyst for aryl–aryl coupling reactions. *Adv. Synth. Catal.* **346**(13–15), 1812–1817 (2004)
2. G. Bringmann, R. Walter, R. Weirich, The directed synthesis of biaryl compounds: modern concepts and strategies. *Angew. Chem. Int. Ed. Engl.* **29**(9), 977–991 (1990)
3. C.Y. Hong, N. Kado, L.E. Overman, Asymmetric synthesis of either enantiomer of opium alkaloids and morphinans. Total synthesis of (-)- and (+)-dihydrocodeinone and (-)- and (+)-morphine. *J. Am. Chem. Soc.* **115**(23), 11028–11029 (1993)
4. A.G. Myers, N.J. Tom, M.E. Fraley, S.B. Cohen, D.J. Madar, A convergent synthetic route to (+)-dymenicin A and analogs of wide structural variability. *J. Am. Chem. Soc.* **119**(26), 6072–6094 (1997)
5. S.J. Danishefsky, J.J. Masters, W.B. Young, J.T. Link, L.B. Snyder, T.V. Magee, D.K. Jung, R.C. Isaacs, W.G. Bornmann, C.A. Alaimo, C.A. Coburn, M.J. Di Grandi, Total synthesis of baccatin III and taxol. *J. Am. Chem. Soc.* **118**(12), 2843–2859 (1996)
6. F. Al Momani, D.W. Smith, M.G. El-Din, Degradation of cyanobacteria toxin by advanced oxidation processes. *J. Hazard. Mater.* **150**(2), 238–249 (2008)
7. Y.P. Li, H.B. Cao, C.M. Liu, Y. Zhang, Electrochemical reduction of nitrobenzene at carbon nanotube electrode. *J. Hazard. Mater.* **148**(1–2), 158–163 (2007)
8. A. Mittal, J. Mittal, A. Malviya, D. Kaur, V.K. Gupta, Adsorption of hazardous dye crystal violet from wastewater by waste materials. *J. Colloid Interface Sci.* **343**(2), 463–473 (2010)
9. T. Zeng, Y.P. Chin, W.A. Arnold, Potential for abiotic reduction of pesticides in prairie pothole porewaters. *Environ. Sci. Technol.* **46**(6), 3177–3187 (2012)
10. T. Zeng, K.L. Ziegelgruber, Y.P. Chin, W.A. Arnold, Pesticide processing potential in prairie pothole porewaters. *Environ. Sci. Technol.* **45**(16), 6814–6822 (2011)
11. M. Sohail, J. Huang, Z. Lai, Y. Cao, S. Ruan, M.N. Shah, F.U. Khan, H.I.A. Qazi, B. Ullah, Synthesis of flower-like Co₉S₈/reduced graphene oxide nanocomposites and their photocatalytic performance. *J. Inorg. Organomet. Polym. Mater.* **30**(12), 5168–5179 (2020)
12. N. Marzari, D. Vanderbilt, A. De Vita, M.C. Payne, Thermal contraction and disordering of the Al (110) surface. *Phys. Rev. Lett.* **82**(16), 3296 (1999)
13. H.J. Monkhorst, J.D. Pack, Special points for Brillouin-zone integrations. *Phys. Rev. B.* **13**(12), 5188 (1976)
14. J.P. Perdew, K. Burke, M. Ernzerhof, Fluid vesicles in shear flow. *Phys. Rev. Lett.* **77**, 3865–3868 (1996)
15. G. Zanti, D. Peeters, DFT study of small palladium clusters Pd_n and their interaction with a CO ligand (n = 1–9). *Eur. J. Inorg. Chem.* **2009**(26), 3904–3911 (2009)
16. L.L. Wang, D.D. Johnson, Shear instabilities in metallic nanoparticles: hydrogen-stabilized structure of Pt₃₇ on carbon. *J. Am. Chem. Soc.* **129**(12), 3658–3664 (2007)
17. J.A. Yan, M.Y. Chou, Oxidation functional groups on graphene: structural and electronic properties. *Phys. Rev. B.* **82**(12), 125403 (2010)
18. C.J. Pickard, F. Mauri, All-electron magnetic response with pseudopotentials: NMR chemical shifts. *Phys. Rev. B.* **63**(24), 245101 (2001)
19. U. Ravon, G. Chaplais, C. Chizallet, B. Seyyedi, F. Bonino, S. Bordiga, N.F. Bats, D. Arrusseng, Investigation of acid centers in MIL-53 (Al, Ga) for Brønsted-type catalysis: in situ FTIR and ab initio molecular modeling. *ChemCatChem* **2**(10), 1235–1238 (2010)
20. W.S. Hummers Jr., R.E. Offeman, Preparation of graphitic oxide. *J. Am. Chem. Soc.* **80**(6), 1339–1339 (1958)
21. K. Niedermann, J.M. Welch, R. Koller, J. Cvengroš, N. Santschi, P. Battaglia, A. Togni, New hypervalent iodine reagents for electrophilic trifluoromethylation and their precursors: synthesis, structure, and reactivity. *Tetrahedron* **66**(31), 5753–5761 (2010)
22. S. Santra, K. Dhara, P. Ranjan, P. Bera, J. Dash, S.K.A. Mandal, supported palladium nanocatalyst for copper free acyl Sonogashira reactions: one-pot multicomponent synthesis of N-containing heterocycles. *Green. Chem.* **13**(11), 3238–3247 (2011)
23. J.S. Carey, D. Laffan, C. Thomson, M.T. Williams, Analysis of the reactions used for the preparation of drug candidate molecules. *Org. Biomol. Chem.* **4**(12), 2337–2347 (2006)
24. M.E. Matheron, M. Porchas, Activity of boscalid, fenhexamid, fluazinam, fludioxonil, and vinclozolin on growth of *Sclerotinia minor* and *S. sclerotiorum* and development of lettuce drop. *Plant. Dis.* **88**(6), 665–668 (2004)
25. S. Lebaschi, M. Hekmati, H. Veisi, Green synthesis of palladium nanoparticles mediated by black tea leaves (*Camellia sinensis*) extract: catalytic activity in the reduction of 4-nitrophenol and Suzuki–Miyaura coupling reaction under ligand-free conditions. *J. Colloid Interface. Sci.* **485**, 223–231 (2017)
26. H. Veisi, A. Khazaei, M. Safaei, D. Kordestani, Synthesis of biguanide-functionalized single-walled carbon nanotubes (SWCNTs) hybrid materials to immobilized palladium as new recyclable heterogeneous nanocatalyst for Suzuki–Miyaura coupling reaction. *J. Mol. Catal. A Chem.* **382**, 106–113 (2014)
27. H. Veisi, R. Masti, D. Kordestani, M. Safaei, O. Sahin, Functionalization of fullerene (C₆₀) with metformine to immobilized palladium as a novel heterogeneous and reusable nanocatalyst in the Suzuki–Miyaura coupling reaction at room temperature. *J. Mol. Catal. A Chem.* **385**, 61–67 (2014)
28. H. Veisi, M. Ghadermazi, A. Naderi, Biguanidine-functionalized chitosan to immobilize palladium nanoparticles as a novel, efficient and recyclable heterogeneous nanocatalyst for Suzuki–Miyaura coupling reactions. *Appl. Organomet. Chem.* **30**(5), 341–345 (2016)
29. M. Fang, K. Wang, H. Lu, Y. Yang, S. Nutt, Covalent polymer functionalization of graphene nanosheets and mechanical properties of composites. *J. Mater. Chem.* **19**(38), 7098–7105 (2009)
30. P.V. Kamat, Graphene-based nanoarchitectures. Anchoring semiconductor and metal nanoparticles on a two-dimensional carbon support. *J. Phys. Chem. Lett.* **1**(2), 520–527 (2010)
31. X. Mei, H. Zheng, J. Ouyang, Ultrafast reduction of graphene oxide with Zn powder in neutral and alkaline solutions at room temperature promoted by the formation of metal complexes. *J. Mater. Chem.* **22**(18), 9109–9116 (2012)
32. S. Navalon, A. Dhakshinamoorthy, M. Alvaro, H. Garcia, Carbocatalysis by graphene-based materials. *Chem. Rev.* **114**(12), 6179–6212 (2014)
33. J. Pyun, Graphene oxide as catalyst: application of carbon materials beyond nanotechnology. *Angew. Chem. Int. Ed. Engl.* **50**(1), 46–48 (2011)

34. X. Fan, G. Zhang, F. Zhang, Multiple roles of graphene in heterogeneous catalysis. *Chem. Soc. Rev.* **44**(10), 3023–3035 (2015)
35. M.O. Senge, M. Fazekas, E.G. Notaras, W.J. Blau, M. Zawadzka, O.B. Locos, E.M. Ni-Mhuirheartaigh, Nonlinear optical properties of porphyrins. *Adv. Mater.* **19**(19), 2737–2774 (2007)
36. V.S. Lin, S.G. DiMugno, M.J. Therien, Highly conjugated, acetylenyl bridged porphyrins: new models for light-harvesting antenna systems. *Science* **264**(5162), 1105–1111 (1994)
37. R. Ebrahimi, M. Mohammadi, A. Maleki, A. Jafari, B. Shahmoradi, R. Rezaee, M. Safari, H. Daraei, O. Giah, K. Yetilmezsoy, S.H. Puttaiah, Photocatalytic degradation of 2,4-dichlorophenoxyacetic acid in aqueous solution using Mn-doped ZnO/graphene nanocomposite under LED radiation. *J. Inorg. Organomet. Polym. Mater.* **30**(3), 923–934 (2020)
38. B.F. Machado, P. Serp, Graphene-based materials for catalysis. *Catal. Sci. Technol.* **2**(1), 54–75 (2012)
39. E.A. Kataev, M. Ramana Reddy, G. Niranjana Reddy, V. Hanuman Reddy, C. Suresh Reddy, B.V. Subba Reddy, *New J. Chem.* **40**, 1693 (2016)
40. G. Crini, *Chem. Rev.* **114**, 10940 (2014)
41. A.C. Franzoi, I.C. Vieira, C.W. Scheeren, J. Dupont, *Electroanal.* **22**(1376), 11 (2010)
42. C. Folch-Cano, M. Yazdani-Pedram, C. Olea-Azar, *Molecules* **19**, 14066 (2014)
43. V.B. Yadav, P. Rai, H. Sagir, A. Kumar, I.R. Siddiqui, *New J. Chem.* **42**, 628 (2018)
44. C.P. da Silva, A.C. Franzoi, S.C. Fernandes, J. Dupont, I.C. Vieira, *Enzyme Microb. Technol.* **52**, 296 (2013)
45. M.L. Bender, M. Komiyama, *Cyclodextrins chemistry* (Springer Verlag, Berlin, 1978), p. 96
46. H. Sagir, P.R. Rahila, P.K. Singh, I.R. Siddiqui, *New J. Chem.* **40**, 6819 (2016)
47. I. Abulkalam Azath, P. Suresh, K. Pitchumani, *New J. Chem.* **36**, 2334 (2012)
48. D. Duchêne, *Cyclodextrins and their industrial uses* (Éditions de Santé, Paris, 1987), p. 447
49. E. Bilensoy, *Cyclodextrins in pharmaceuticals, cosmetics and biomedicine; In current and future industrial applications* (Wiley, Hoboken, 2011), p. 440
50. M.K. Rabchinskii, A.T. Dideikin, D.A. Kirilenko, M.V. Baidakova, V.V. Shnitov, F. Roth, S.V. Konyakhin, N.A. Besedina, S.I. Pavlov, R.A. Kuricyn, N.M. Lebedeva, Facile reduction of graphene oxide suspensions and films using glass wafers. *Sci. Rep.* **8**(1), 1–11 (2018)
51. A. Romero, M.P. Lavin-Lopez, L. Sanchez-Silva, J.L. Valverde, A. Paton-Carrero, Comparative study of different scalable routes to synthesize graphene oxide and reduced graphene oxide. *Mater. Chem. Phys.* **203**, 284–292 (2018)
52. Y. Gao, G. Li, Z. Zhou, L. Guo, X. Liu, Supramolecular assembly of poly (β -cyclodextrin) block copolymer and benzimidazole-poly (ϵ -caprolactone) based on host-guest recognition for drug delivery. *Colloids. Surf. B: Biointerfaces.* **160**, 364–371 (2017)
53. K. Javanmiri, R. Karimian, Green synthesis of benzimidazoloquinazolines and 1, 4-dihydropyridines using magnetic cyanoguanidine-modified chitosan as an efficient heterogeneous nanocatalyst under various conditions. *Monatsh. Chem.* **151**(2), 199–212 (2020)
54. B. Bananezhad, M.R. Islami, E. Ghonchehpour, H. Mostafavi, A.M. Tikdari, H.R. Rafiei, Bentonite clay as an efficient substrate for the synthesis of the super stable and recoverable magnetic nanocomposite of palladium (Fe_3O_4 /Bentonite-Pd). *Polyhedron* **162**, 192–200 (2019)
55. R. Pernites, A. Vergara, A. Yago, K. Cui, R. Advincula, Facile approach to graphene oxide and poly (N-vinylcarbazole) electro-patterned films. *Chem. Commun.* **47**(35), 9810–9812 (2011)
56. C.C. Wang, D.H. Chen, T.C. Huang, Synthesis of palladium nanoparticles in water-in-oil microemulsions. *Colloids. Surf. A Physicochem. Eng. Asp.* **189**(1–3), 145–154 (2001)
57. R.M. Sarfraz, M. Ahmad, A. Mahmood, M.R. Akram, A. Abrar, Development of β -cyclodextrin-based hydrogel microparticles for solubility enhancement of rosuvastatin: an in vitro and in vivo evaluation. *Drug Des. Devel. Ther.* **11**, 3083 (2017)
58. S. Mizuno, T.A. Asoh, Y. Takashima, A. Harada, H. Uyama, Palladium nanoparticle loaded β -cyclodextrin monolith as a flow reactor for concentration enrichment and conversion of pollutants based on molecular recognition. *Chem. Commun.* **56**(92), 14408–14411 (2020)
59. Y. Zhang, B. Hu, X.M. Cao, L. Luo, Y. Xiong, Z.P. Wang, X. Hong, S.Y. Ding, β -Cyclodextrin polymer networks stabilized gold nanoparticle with superior catalytic activities. *Nano Res.* **14**(4), 1018–1025 (2021)

Publisher's Note Springer Nature remains neutral with regard to jurisdictional claims in published maps and institutional affiliations.